

## Field guide of Izu-Oshima Volcano

Takahiro Yamamoto<sup>1,\*</sup>

Takahiro Yamamoto (2017) Field guide of Izu-Oshima Volcano. *Bull. Geol. Surv. Japan*, vol.68 (4), p. 163–175, 18 figs.

**Abstract:** Izu-Oshima volcano is an active basaltic stratovolcano in the Izu-Mariana arc, and its last major eruption occurred in 1986. This field guide includes descriptions about the 1986 products, the Miharayama Central Cone, the 1421? product at the southern coast, the 1.7-ka caldera-forming products, the pre-caldera tephra formation and the 2013 lahar.

**Keywords:** Izu-Oshima volcano, 1986 eruption, Miharayama, caldera

### 1. Introduction

Izu-Oshima volcano is an active basaltic stratovolcano that forms the northernmost island (15×9 km) of the Izu-Mariana arc (Fig. 1). The elevation of this island is 764 m a.s.l., but the volcanic edifice height is over 1,000 m from the sea floor. The island consists of highly dissected remnants of three old (Early Pleistocene) volcanoes, which are exposed on the northern and eastern coasts, as well as in the products of Izu-Oshima volcano proper (Isshiki, 1984; Fig. 2). These products cover the older edifices and occupy most of the subaerial portion of the island.

### 2. Eruption history

Izu-Oshima volcano is composed of lava flows and volcaniclastic rocks of low-K, arc-type tholeiitic olivine basalt and pyroxene-olivine basalt (Kawanabe, 1991). The older edifice of the volcano is called the Senzu Group (Nakamura, 1964) and is made up of phreatomagmatic coarse ejecta and lahar deposits with a small amount of lava flows (Fig. 2). Volcanic activity started at about 40 to 50 ka, and represents the stage of emergence of an island. The younger edifice of the volcano consists of normal subaerial alternations of lava flows and scoria and ash falls. This activity began about 20 ka and marks the stage of continuous growth of a stratovolcano above sea level. The upper unit is subdivided into pre-caldera and syn- and post-caldera deposits (Nakamura, 1964). The pre-caldera deposits are made up of about 100 layers of pyroclastic deposits. The intervals between the layers are presumably 150 years on average. There are many flank volcanoes forming fissures, scoria cones and tuff cones. Zone of the flank vents is elongated in NNW to SSE that reflects a regional stress field.

At about 1.7 ka, after a scoria eruption from the summit

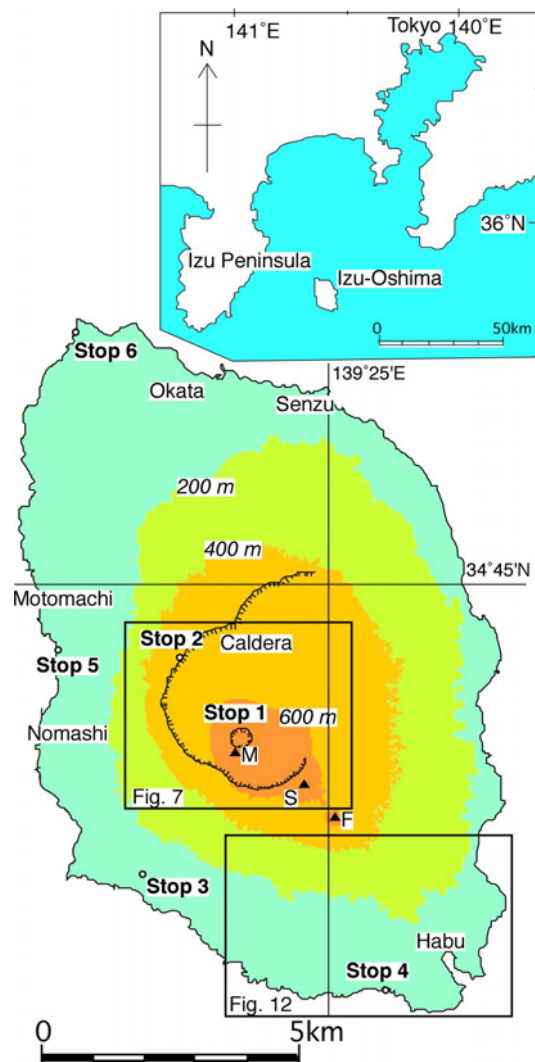


Fig. 1 Index map of Izu-Oshima volcano. M = Miharayama; S = Shiroishiyama; F = Futagoyama

<sup>1</sup> AIST, Geological Survey of Japan, Research Institute of Earthquake and Volcano Geology

\* Corresponding author: T. Yamamoto, Central 7, 1-1-1 Higashi, Tsukuba, Ibaraki 305-8567, Japan. Email: t-yamamoto@aist.go.jp

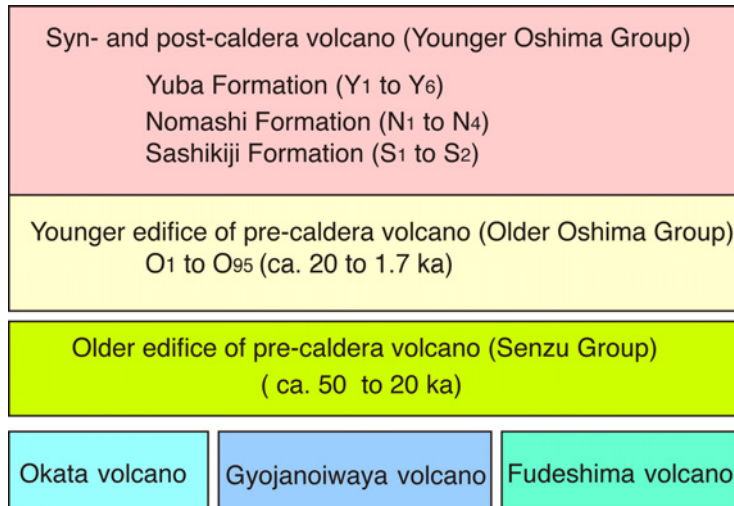


Fig. 2 Geological summary of Izu-Oshima island. Modified from Kawanabe (1998).

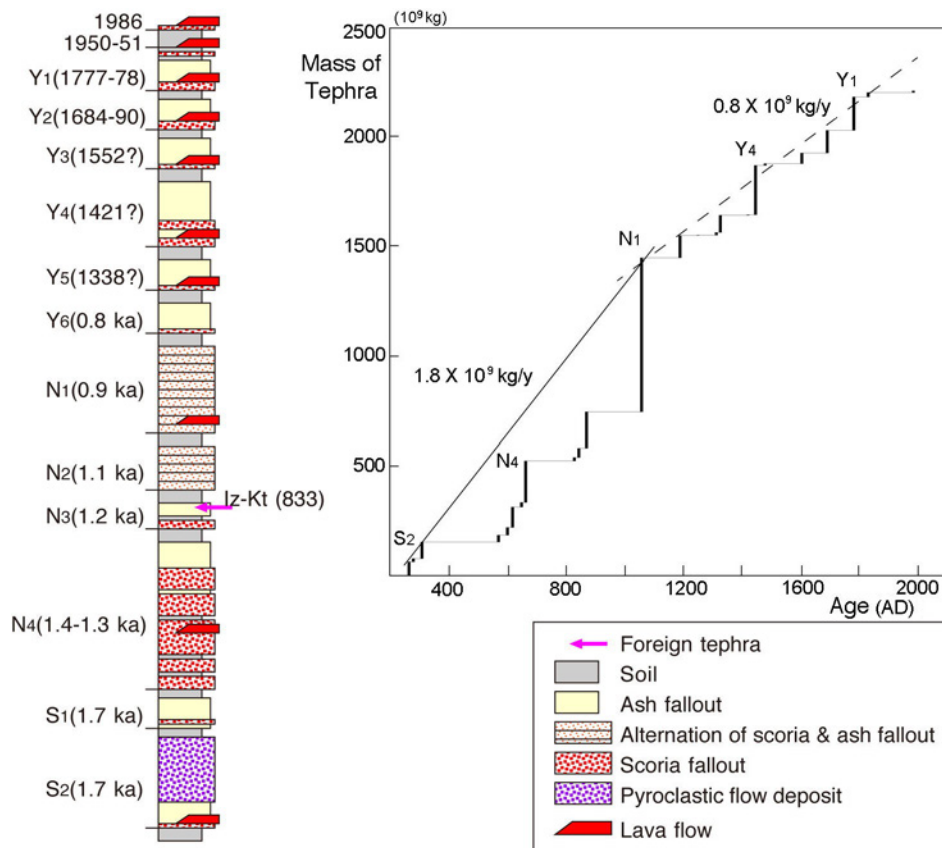


Fig. 3 Stratigraphic section and cumulative mass of tephra for the syn- and post-caldera products of Izu-Oshima volcano. Iz-Kt = Izu-Kozushima-Tenjosan tephra (biotite rhyolite) from Kozushima volcano at AD833. Modified from Kawanabe (1998; 2012).

and several flank eruptions, a large phreatic explosion occurred in the summit area and high-speed pyroclastic density current covered almost all the entire island (Yamamoto, 2006; S<sub>2</sub> in Figs. 2 and 3). The present shape of the summit caldera is thought to be formed in this syn-

caldera stage (Sashikiji Formation; Nakamura, 1964). The post-caldera products are composed of 10 large eruptions and several minor ones (Koyama and Hayakawa, 1996; Kawanabe, 2012). Nakamura (1964) has divided into the Nomashi and Yuba Formations across an erosional contact

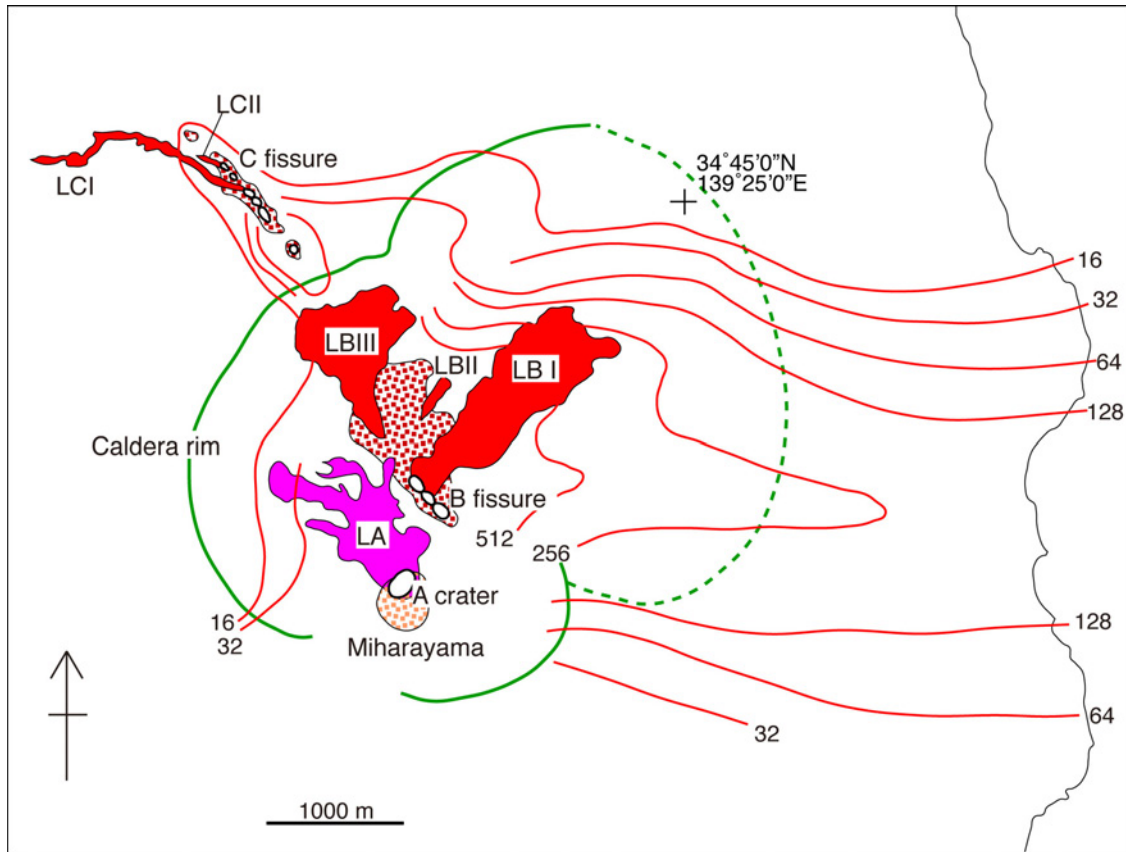


Fig. 4 Distribution of the products of the 1986 eruption. Numerals of each isopach are the thickness of the scoria fall deposits in millimeters. LA, LBI, LBII, LBIII, LCI and LCII are names of lava flows. Hatched areas are scoria cones. Mt Mihara (Miharayama) is the central cone within the summit caldera. Modified from Soya *et al.* (1987).

(Fig. 2). The eruptive volume of these large eruptions is up to a cubic kilometer and the average recurrent interval of the large ones is 100 to 150 years (Fig. 3). The most recent large eruption occurred in 1777–78 ( $Y_1$ ). Large-scale eruptions usually began with scoria fall deposition followed by effusion of lava flows. In some events, flank eruptions took place and caused violent phreatomagmatic explosions near the coast. The emission of phreatic ash from the central cone, Miharayama, followed for several years after the early magmatic activity. After the  $Y_1$  eruption, many medium- to small-scale eruptions occurred. The 1876–77, 1912–14, 1950–51 and 1986–87 eruptions were relatively large and erupted several tens million cubic meters of magma.

### 3. The 1986 eruption

The 1986 event began with a strombolian eruption and basalt lava effusion from the A crater in Miharayama Central Cone on 15 November (Figs. 4 and 5). On 21 November, after a short repose of activity, a fissure eruption occurred with sub-plinian plumes in the northwestern caldera floor (B fissure). The plumes reached 8,000 m height and sprayed scoria fallout on the eastern side. As



Fig. 5 The 1986 strombolian summit eruption from the A crater accompanied by lava flows. Viewed from the NW (Gojinkajaya). Photo by S. Nakano, 21 November 1986.

fissure extended outside the caldera (C fissure) and lava flow (LCI) rushed to the largest town, Motomachi, whole residents and visitors were evacuated out of the island. The ejecta from B and C fissures was andesite, which differed from one of A crater in origin. The eruption itself ceased in the morning of 22 November, but evacuation lasted for about one month. On 16 November 1987,

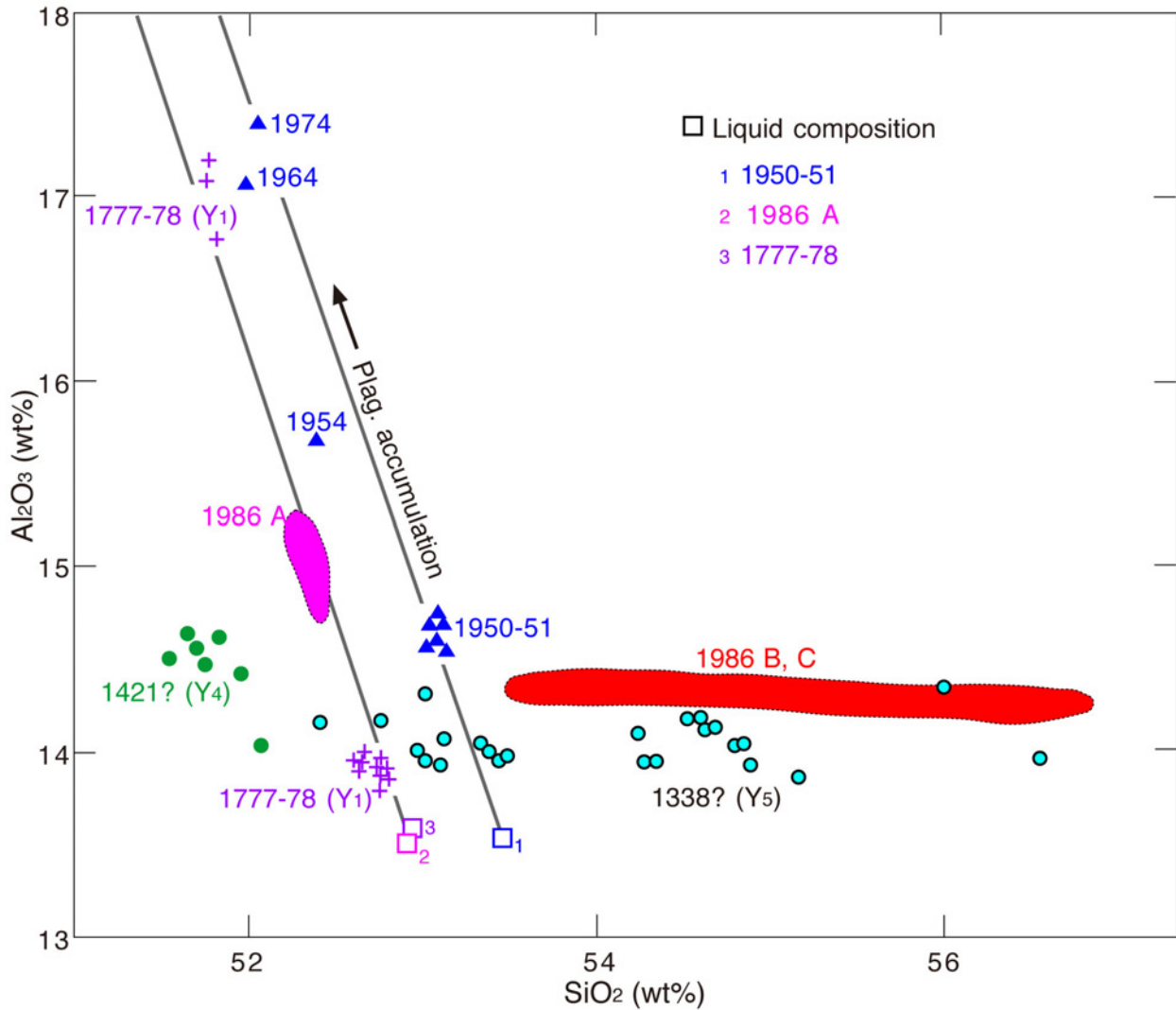


Fig. 6  $\text{Al}_2\text{O}_3$  vs.  $\text{SiO}_2$  diagram of products of the 1338, 1421, 1777–1778, 1950–1974 and 1986 eruptions; 1986A designates the 1986 summit eruption and 1986B, C the 1986 flank eruption. Three open squares indicate the calculated liquid compositions. Two lines denote respective plagioclase-control lines connected with plagioclase. After Nakano and Yamamoto (1991).

with loud explosions, the lava filling the old pit crater in Miharayama Central Cone were exploded and collapsed. Afterward, several collapses were accompanied by small eruptions, recreating the pit crater in Miharayama. No surface activity, but fumaroles have occurred since the small eruption of 4 October 1990. However, earthquake and volcanic tremor are sometimes observed and a slow inflation of the volcano continues.

#### 4. Geochemistry of the products

The magma of this volcano consists of two types (Nakano and Yamamoto, 1991). One is “plagioclase-controlled” and the other is “differentiated” magma (multimineral-controlled); i.e. the bulk chemistry of the first magma type is controlled by plagioclase addition or

removal, while that of the second type is controlled by fractionation of plagioclase, orthopyroxene, clinopyroxene, and titanomagnetite (Fig. 6). Summit eruptions of this volcano tap only plagioclase-controlled magmas, while flank eruptions supply both magma types. It is considered unlikely that both magma types would coexist in the same magma chamber based on the petrology. In the case of the 1986 eruption, the flank magma was isolated from the summit magma chamber or central conduit, and formed small magma pockets, where further differentiation occurred due to relatively rapid cooling. In a period of quiescence prior to the 1986 eruption, new magma was supplied to the summit magma chamber, and the summit eruption began. The dike intrusion or fracturing around the small magma pockets triggered the flank eruption of the differentiated magma.

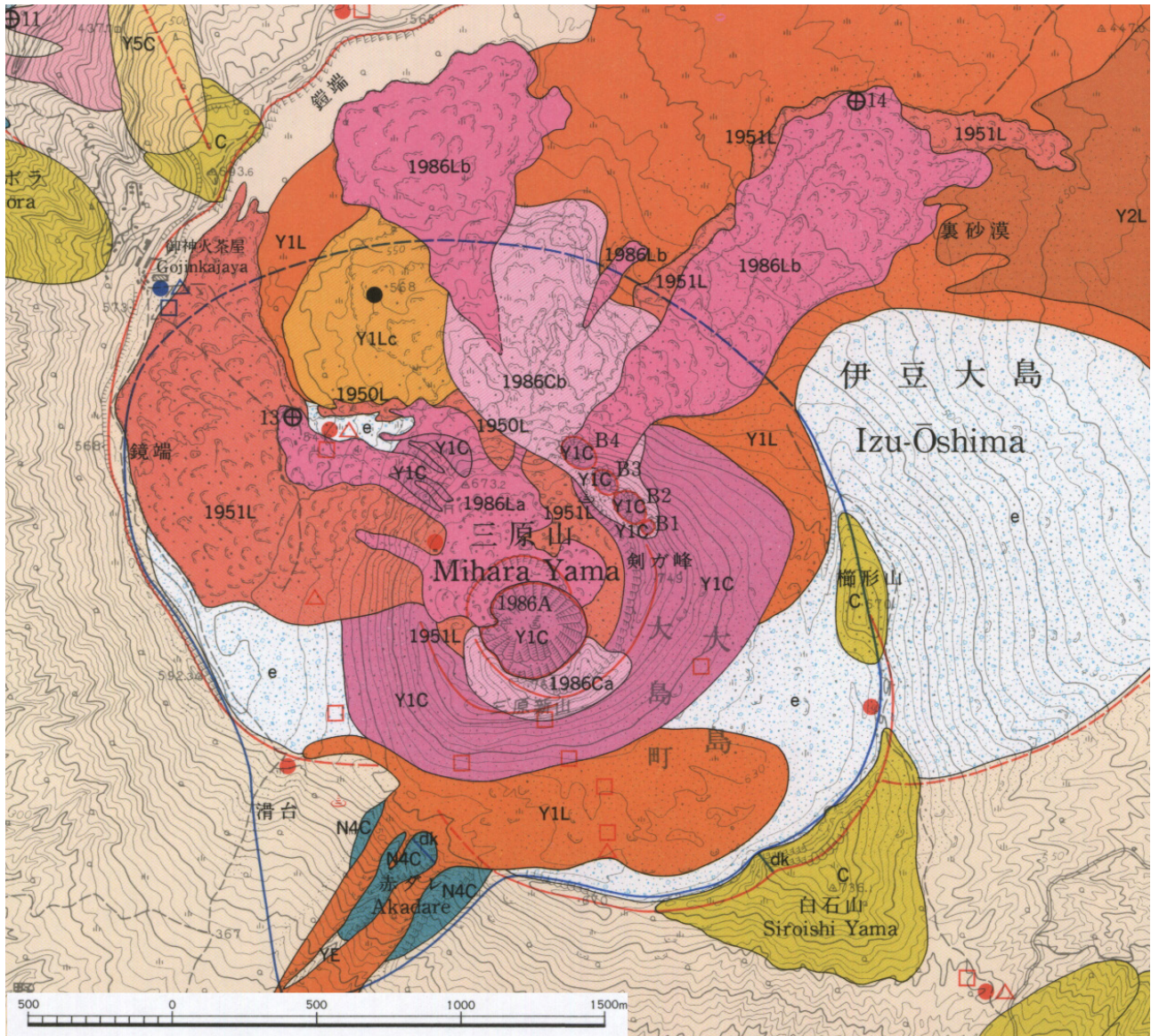


Fig. 7 Geological map around Miharayama Central Cone. Part of the map by Kawanabe (1998).

## 5. Description of field stops

**Stop 1: Hike to Miharayama Central Cone** (34.73716°N, 139.37996°E to 34.72420°N, 139.39511°E)

There is a trail from Gojinkajaya on the caldera-rim to the top of Miharayama. We can observe the 1986, 1950–1951, Y<sub>1</sub> (1777–1778) and Y<sub>2</sub> (1684) products along this trail (Fig. 7).

The 1986 eruption occurred at the summit from 15 to 23 November (A crater) and at the fissure vents both inside (B fissure) and outside the caldera (C fissure) on 21 November (Fig. 4). The summit lava (1986La) is augite-pigeonite-bronzite basalt, with 6 to 8% plagioclase phenocrysts. Mafic phenocrysts of 1986La total less than 1%. The flank lava (1986Lb and 1986Lc) is nearly aphyric andesite, with rare phenocrysts of plagioclase,

orthopyroxene, clinopyroxene and titanomagnetite, that total less than 1% modally. 1986La is chemically homogeneous throughout the eruption, with 52.2 to 52.5% SiO<sub>2</sub> and approximately 15% Al<sub>2</sub>O<sub>3</sub>, while flank lavas show a wide variation of SiO<sub>2</sub> ranging from 53.5 to 56.9% (Fig. 6). The Al<sub>2</sub>O<sub>3</sub> content of the flank lavas is nearly constant (14.2 to 14.4%), in spite of the SiO<sub>2</sub> variation. Temporal variation of the B scoria showed that, initially, scoria compositions were bimodal; i.e. between 53.5 and 53.9% and between 55.3 and 56.1% SiO<sub>2</sub>. The SiO<sub>2</sub>-rich scoria was, however, restricted to the initial stage. These temporal compositional variations imply a compositional zonation in the flank magma chamber (Nakano and Yamamoto, 1991).

The 1950–1951 eruption was an intermediate-scale eruption at Miharayama Central Cone similar to the 1986

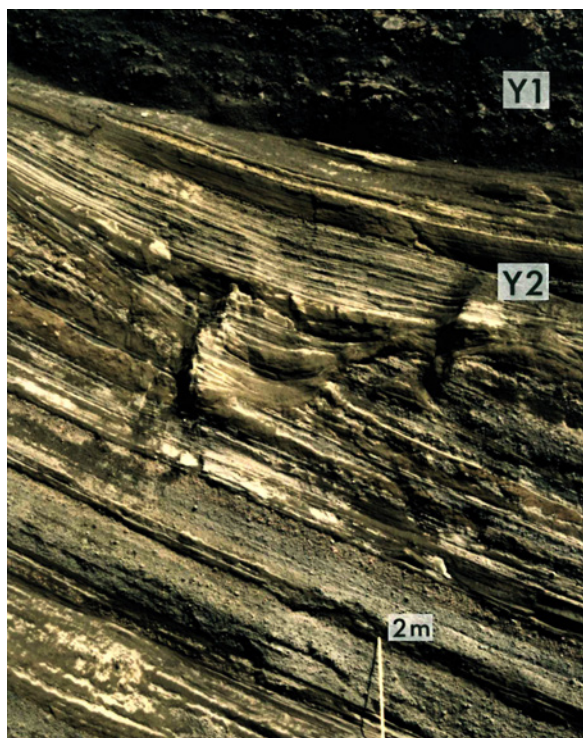


Fig. 8 Phreatomagmatic fallout and surge deposits caused by water inflow into the Miharayama conduit during the magma-withdrawal stage of the  $Y_2$  Member ( $Y_2$ ) at the B2 crater in Miharayama Central Cone (see Fig. 7).  $Y_1$  is the basal scoria fall deposit of the  $Y_1$  Member. After Yamamoto (1994). Photo by 15 March 1992.

summit activity from the A crater. Strombolian eruptions and lava effusions took place from the summit crater (Isshiki, 1984). The 1950–1951 lava is augite-bronzite basalt, with 5 to 10% plagioclase phenocrysts, while mafic phenocrysts constitute much less than 1%. The lava is chemically homogeneous with 14.5 to 14.8%  $Al_2O_3$  and approximately 53%  $SiO_2$  (Fig. 6).

The  $Y_1$  and  $Y_2$  eruptions were large-scale ones, and Miharayama Central Cone is made up mainly of proximal deposits of  $Y_1$  and  $Y_2$  products. Both consist of basal scoria fall deposit by a sub-plinian eruption and overlying alternation of crossbedded pyroclastic surge and scoria-ash fall deposits (Fig. 8). The overlying unit are called as ash-fall stage deposits, and it is interpreted that the pyroclastic surges was caused by ground water inflow into a conduit during withdrawal of magma (Yamamoto, 1994). The pyroclastic surges expanded about 1 km from the summit vent (blue line in Fig. 7). Duration of main eruption stage, start from basal scoria eject to lava effusion, ranges from 1 to 2 weeks in  $Y_2$  eruption, to 14.5 months in  $Y_1$  eruption. Those of magma-withdrawal stage, ash-fall stage, lasted 6 years in  $Y_2$  and 9 years in  $Y_1$ , respectively (Tsukui *et al.*, 2009).

The  $Y_1$  early magma rich in plagioclase phenocrysts was ejected from the central cone. Thereafter, nearly aphyric

lava effused at the base of Miharayama Central Cone. Early ejecta of the  $Y_1$  eruption comprise orthopyroxene basalt, with 18% plagioclase and less than 0.5% orthopyroxene phenocrysts. This tephra contains approximately 17%  $Al_2O_3$  and 52%  $SiO_2$  (Fig. 6). Late lava flows are aphyric basalt, containing less than 2% plagioclase and very rare orthopyroxene and augite phenocrysts. They are chemically homogeneous, containing 52.6 to 52.8%  $SiO_2$  and approximately 14%  $Al_2O_3$  (Nakano and Yamamoto, 1991).

## Stop 2: Caldera-forming ejecta at Gojinkajaya (34.73945°N, 139.38144°E)

The Sashikiji 2 ( $S_2$ ) Member, exposing at Gojinkajaya, was formed by an explosive eruption accompanied with caldera depression at about cal AD 340 (Yamamoto, 2006). The  $S_2$  Member is divided into six units from  $S_2$ -a to  $S_2$ -f in ascending order (Fig. 9). The  $S_2$ -a unit consists of scoria, bomb and aa lava flows from flank fissures. The  $S_2$ -b unit is made up of well-bedded ash and fine-lapilli from the summit. The  $S_2$ -c unit is composed of matrix-supported breccia, locally filling valley bottoms and containing abundant deformed soil fragments and woods (Stop 5). The  $S_2$ -d unit consists of reverse to normal grading, clast-supported breccia with ash matrix, covering topographic relief in the whole island (Stop 2; Figs. 10 and 11). The  $S_2$ -e unit is composed of dune- to parallel-bedded lapilli and ash in the proximal facies. The  $S_2$ -f unit is clast-supported breccia with or without ash matrix. The  $S_2$ -c and -d units are quite different in sedimentological features as follows. The grain fabric measurements have revealed that the  $S_2$ -d unit has a-type imbrication showing the longest axis of grains parallel to the flow direction. On the other hand, the  $S_2$ -c has random fabric of grains. The grain size distribution of the  $S_2$ -d unit shows a bimodal nature having subpopulations at  $\phi$  -1.0 to +1.0 and coarser than  $\phi$  -2.5. The bimodal nature and a-type imbrication suggest that the two transport processes overlap; the load of a turbulent suspension is not all in true suspension as the coarser population may travel in a cast-dispersion mass flow. The  $S_2$ -c unit shows a polymodal grain size distribution with multi subpopulations from coarse to fine. The poor sorting, massive appearance, valley-confined distribution, and random grain fabric of the  $S_2$ -c unit are characteristic of deposition from a cohesive flow without formation of traction-related bedforms or sorting of different grain sizes by turbulence. The modal composition measurements have indicated that the  $S_2$ -c and -d units lack essential scoriaceous or glassy fragments. This evidence indicates that both units are derived from steam explosions due to outburst of highly-pressurized geothermal fluid within the edifice. The  $S_2$ -c unit was plausibly generated by remobilization of phreatic debris around the summit caused by ejection of condensed water from a plume or heavy rainfall. The  $S_2$ -d unit was a pyroclastic density current deposit resulted from collapse of a highly-discharged phreatic plume. Estimated velocities of the

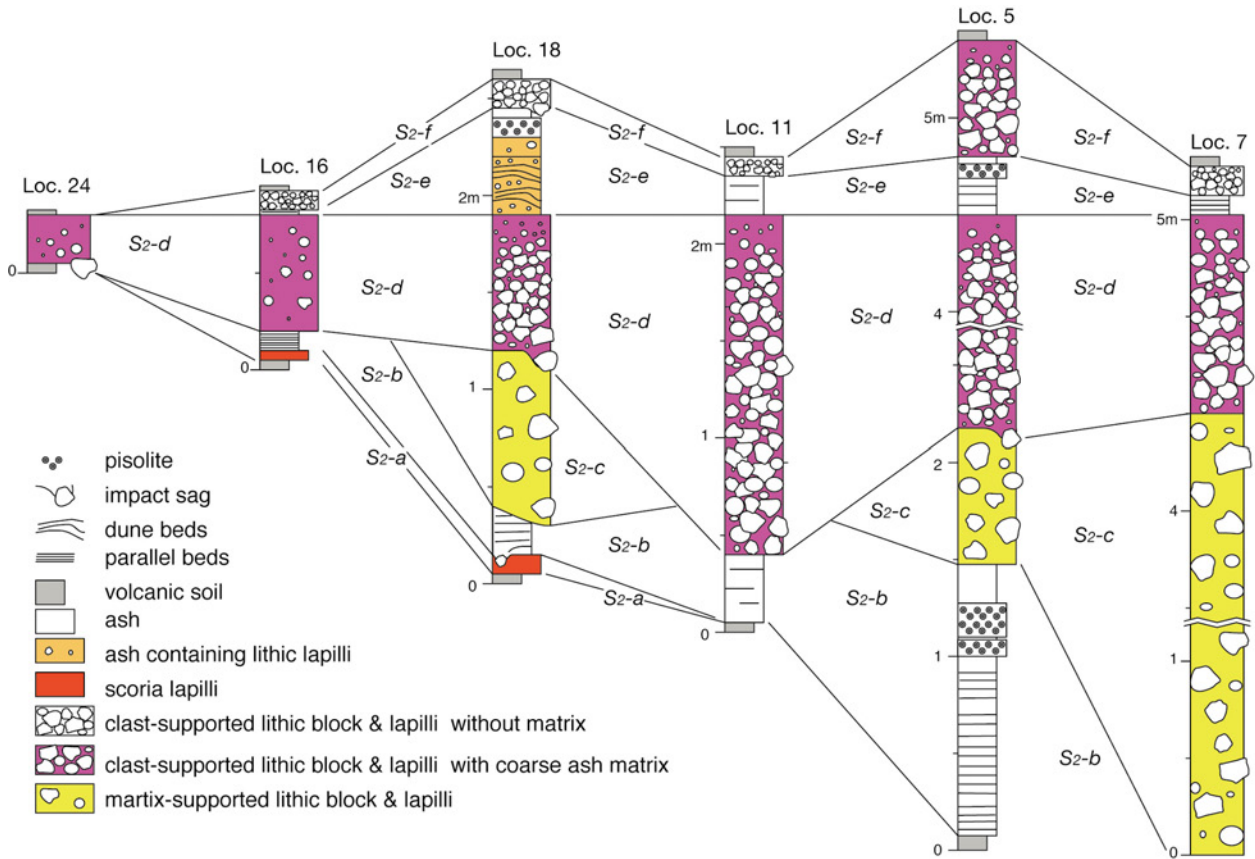


Fig. 9 Stratigraphic columns through the S<sub>2</sub> Member. Loc. 5 = Gojinkajaya (Stop 2). After Yamamoto (2006).



Fig.10 Reverse to normal grading, clast-supported breccia with ash matrix in the S<sub>2</sub>-d unit (Stop 2). This breccia consists of basaltic lithic fragments without an essential material and was emplaced from a high-speed pyroclastic flow. After Yamamoto (2006).



Fig.11 Large cutting made up of abundant pyroclastic fall deposits at Chisodaisetsudanmen. Lithic pyroclastic flow deposit of the S<sub>2</sub>-d unit (S<sub>2</sub>-d) pinches out toward the topographic ridge. Arrows shows impact structures at the bottom of the S<sub>2</sub>-d unit.

current are 150 to 30 m/s based on suspended grain sizes.

### Stop 3: Massive pile of pyroclastic fall deposits at Chisodaisetsudanmen (34.70324°N, 139.37205E)

About 100 pyroclastic fall deposits of the younger edifice (Older Oshima Group) are exposed along road-cuttings along the southwestern coast (Fig. 11). Individual deposits are products of large-scale eruptions from the summit. Most of the deposits consist of basal scoria and overlying ash fall deposits, corresponding to the main eruption and magma-withdrawal stages. The lowest deposits of this cuttings erupted at about 20 ka. There are some unconformities within the pile of fall deposits. However, these unconformities are local and interpreted as erosion surfaces by water flushes.

The S<sub>2</sub>-d lithic pyroclastic flow deposit is intercalated in the upper part of this load-cuttings (Fig. 11). Many impact sags at the base of S<sub>2</sub>-d unit suggest a vigorous explosion during the caldera formation.

### Stop 4: Ejecta from the Y<sub>4</sub> (1421?) fissure at the southern coast, Imasaki (34.68286°N, 139.42441°E)

During the Y<sub>4</sub> event, both summit and flank eruptions took place. The latter occurred along the southern part of the main rift zone (Fig. 12). The flank lava is basalt,

with less than 1% plagioclase and very rare olivine phenocrysts. The chemical compositions of the lava are quite uniform throughout, with SiO<sub>2</sub> ranging from 52.1 to 52.6% and Al<sub>2</sub>O<sub>3</sub> ranging from 14.2 to 14.8% (Fig. 6). The summit lava is also basalt, and contains less than 1% plagioclase and very rare olivine phenocrysts (Nakano and Yamamoto, 1991). The chemistry is similar to that of the contemporaneous flank eruption products.

The stratigraphy of the Y<sub>4</sub> products at Imasaki shows that the flank fissures gradually expanded toward the southeast (Fig. 13). Aa lava flow from the inland Y<sub>4</sub> fissure (Y4L) are covered by partly-welded scoria rampart (Y4C) with feeder dike (Y4D), and topped by tuff breccia containing shattered glassy basalt and lithic fragments from off-shore fissures (Y4T). This Y4T unit makes elongated tuff cone with a broad crater, and generated by interactions between magma and sea water.

### Stop 5: Various lahar deposits at Motomachi (34.74428°N, 139.35563°E)

The Izu-Oshima 2013 lahar (Fig. 14) occurred on the western steep slope of the volcano in response to heavy rain brought by the 26th Typhoon (WIPHA) on 16 October 2013. The lahar damaged Motomachi village, resulting in many fatalities. This lahar deposit consists of moderately

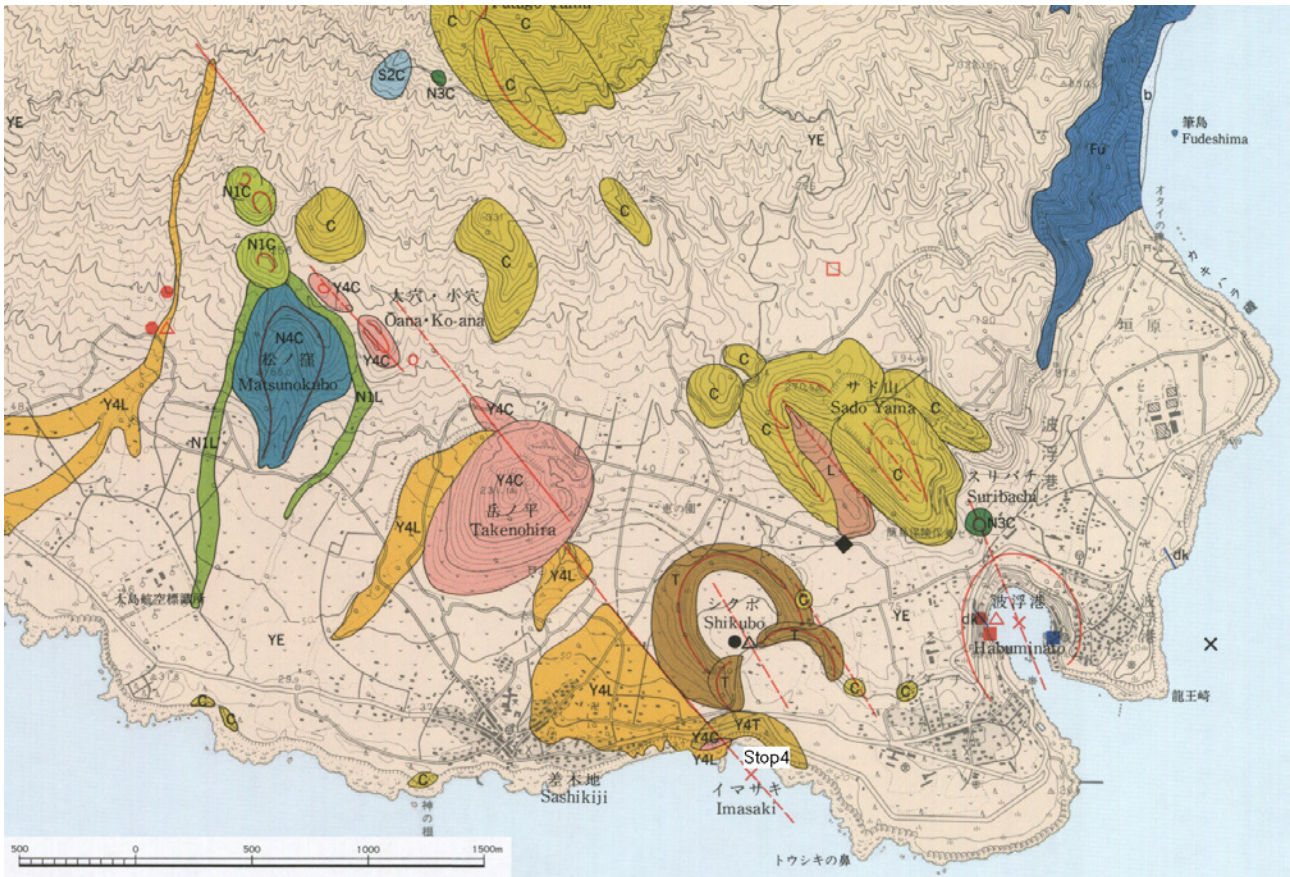


Fig. 12 Geological map of the southern part of Izu-Oshima volcano. Part of the map by Kawanabe (1998).



Fig. 13 Section of the Y<sub>4</sub> products from the southern fissures at Imasaki. Y<sub>4</sub>D = feeder dike of Y<sub>4</sub>; Y<sub>4</sub>L = lava flow of Y<sub>4</sub>; Y<sub>4</sub>C = scoria cone of Y<sub>4</sub>; Y<sub>4</sub>T = tuff cone of Y<sub>4</sub>; YEL = lava flow of Younger Edifice of Pre-Caldera Volcano.

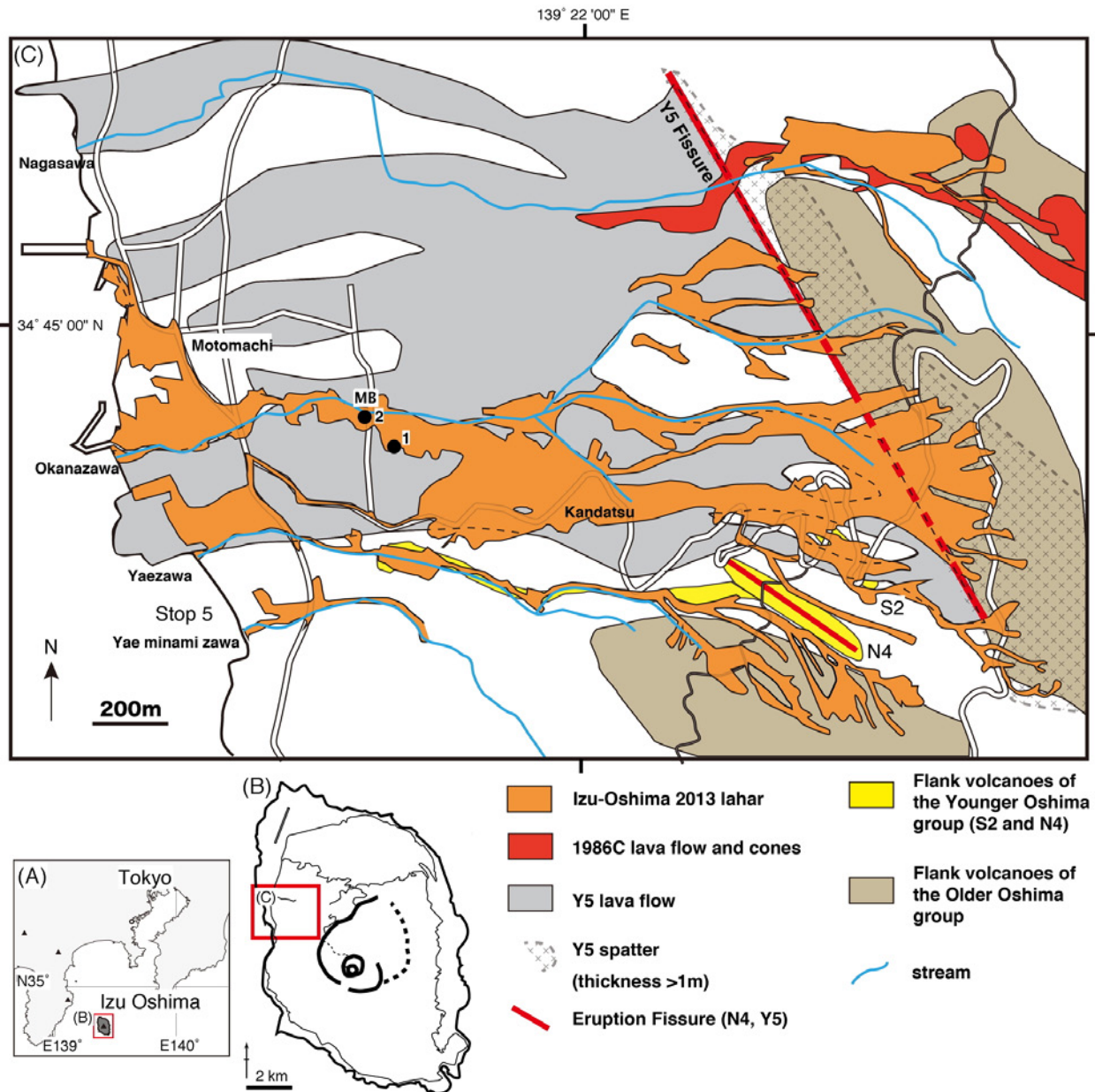


Fig. 14 Distribution of the Izu-Oshima 2013 lahar in the western part of Izu-Oshima volcano. After Yamamoto and Kawanabe (2014).

sorted, coarse- to medium-grained sand with pebbles and well-sorted fine- to very-fine-grained sand. The bi- and uni-modal grain-size distributions of the deposit suggest that the lahar was emplaced as a hyperconcentrated flood flow (Yamamoto and Kawanabe, 2014). This lahar was generated by a shallow-seated slope failure within ash fall deposits covering the Y<sub>5</sub>-stage collapse wall, and it cascaded turbulently down to Motomachi village at high speed spreading on the slope (Fig. 15).

Hyperconcentrated flood flow deposits immediately after the Y<sub>5</sub> eruption and cohesive lahar deposits of the S<sub>2</sub>-c unit are exposed along the southern coast of Motomachi (Stop 5). The earlier deposits are discontinuously bedded pebble and sand containing abundant Y<sub>5</sub> scoria (Fig. 16).

On the other hand, the latter deposits consist of matrix-supported gravel with wood trunks (Fig. 17).

**Stop 6: Unconformity between the older edifice of Pre-caldera Izu-Oshima Volcano and Okata Volcano at Nodahama (34.79723°N, 139.36084°E)**

Pre-caldera Izu-Oshima Volcano started its activity on the sea floor about 30 to 40 ka. The ejecta at this stage were mostly coarse-grained pyroclastic materials in phreatomagmatic origin. In this stop, stratified pyroclastic surge deposits during this stage about the edifice of Okata Volcano (Fig. 18). The surge deposits contain abundant polyhedral-shaped basaltic scoria, indicating a rapid chilling effect by external water. Okata Volcano is deeply-

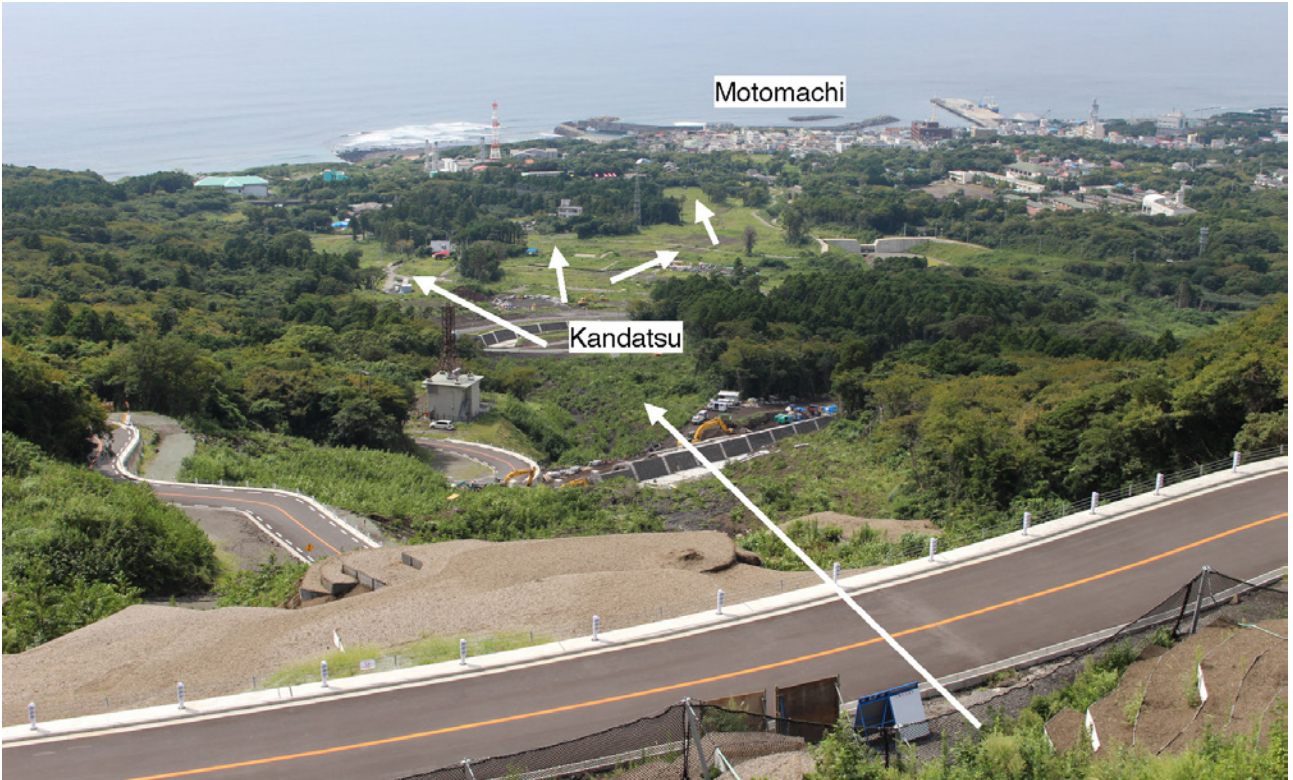


Fig. 15 Downstream path of the 2013 lahar (white arrows) from the Gojinka Sky Line. This lahar cascaded as a sheet flow on this slope and destroyed houses in the Kandatsu village. Photo by 15 September, 2016.



Fig. 16 Hyperconcentrated flow deposits of the Y<sub>5</sub> products at Stop 5. Lithofacies of this lahar deposit are similar to the 2013 ones and poured down the same path.



Fig. 17 Cohesive lahar deposit of the S<sub>2</sub>-c unit (S2-c) filling a channel at Stop 5. This lahar deposit is composed of matrix-supported breccia containing deformed soli fragments and wood trunks. S<sub>1</sub> is the ash fall deposit of the S<sub>1</sub> Member.



Fig. 18 Unconformity between the older edifice of Pre-caldera Izu-Oshima Volcano (OE) and Okata Volcano (Ok) at Nodahama (Stop 6).

dissected stratovolcano in the northern part of the island and composed of mainly basaltic lava flows, pyroclastic rocks, and dikes. The age of Okata Volcano is uncertain, but probably Early Pleistocene.

#### Acknowledgements

This field guide was made for the excursion of International Workshop on Petrological Analysis of Pre-eruptive Magma Processes (AIST Tsukuba Central, November 9, 2016). I would like to thank Shun Nakano, Akiko Tanaka and Yoshihisa Kawanabe for their comments.

#### References

- Isshiki, N. (1984) *Geology of the O Shima district*. With geological sheet map at 1 : 50,000, Geological Survey of Japan, 133p. (in Japanese with English abstract)
- Kawanabe, Y. (1991) Petrological evolution of Izu Oshima volcano. *Bulletin of Volcanological Society of Japan*, **36**, 297–310. (in Japanese with English abstract)
- Kawanabe, Y. (1998) *Geological map of Izu-Oshima volcano*. Geological Survey of Japan.
- Kawanabe, Y. (2012) New <sup>14</sup>C ages of the Younger Oshima Group, Izu-Oshima volcano, Izu-Ogasawara arc, Japan. *Bulletin of Geological Survey of Japan*, **63**, 283–289. (in Japanese with English abstract)
- Koyama, M. and Hayakawa, Y. (1996) Syn- and post-caldera eruption history of Izu Oshima volcano based on tephra and loess stratigraphy. *Journal of Geography (Chigakuzasshi)*, **105**, 133–162. (in Japanese with English abstract)
- Nakamura, K. (1964) Volcano-stratigraphic study of Oshima volcano, Izu. *Bulletin of Earthquake Research Institute, University of Tokyo*, **42**, 649–728.
- Nakano, S. and Yamamoto, T. (1991) Chemical variations of magmas at Izu-Oshima volcano, Japan: Plagioclase-controlled and differentiated magmas. *Bulletin of Volcanology*, **53**, 112–120.
- Soya, T., Sakaguchi, K., Uto, K., Nakano, S., Hoshizumi, H., Kamata, H., Sumii, T., Kaneko, N., Yamamoto, T., Tsuchiya, N., Suto, S., Yamazaki, H., Yamaguchi, Y., Okumura, K. and Togashi, S. (1987) The 1986 eruption and products of Izu-Oshima volcano. *Bulletin of Geological Survey of Japan*, **38**, 609–630. (in Japanese with English abstract)
- Tsukui, M., Dangi, K., Sato, S. and Hayashi, K. (2009) Izu-Oshima volcano: precise sequence and mitigation program of the latest three large-scale eruptions revealed by historical documents. *Bulletin of Volcanological Society of Japan*, **54**, 93–112. (in Japanese with English abstract)
- Yamamoto, T. (1994) Phreatomagmatic explosions: basic problems of dynamic interactions between magma and water. *Memories of Geological Society of Japan*, no.43, 63–72. (in Japanese with English abstract)
- Yamamoto, T. (2006) Pyroclastic density current from the caldera-forming eruption of Izu-Oshima volcano, Japan: Restudy of the Sashikiji 2 Member based on stratigraphy, lithofacies, and eruption age. *Bulletin of Volcanological Society of Japan*, **51**, 257–271. (in Japanese with English abstract)
- Yamamoto, T. and Kawanabe, Y. (2014) Sedimentary characteristics of the Izu-Oshima 2013 lahar: classification of various lahar deposits based on grain-size distribution. *Journal of Geological Society of Japan*, **120**, 233–245. (in Japanese with English abstract)

Received December 5, 2016

Accepted March 7, 2017

Available on-line June 29, 2017

## 伊豆大島火山巡検ガイド

山元孝広

### 要 旨

この地質ガイドは、2016年11月に開催された噴火準備過程の岩石学的解析に関する国際ワークショップの伊豆大島巡検のために作成されたものである。見学地点では、1986年噴出物、三原山火砕丘、南海岸の1421?年噴出物、1.7千年前のカルデラ形成期噴出物、先カルデラ期のテフラ層や、2013年ラハールが観察できる。

